

Electronic Supplementary Information (ESI) for

Donor–Acceptor Polymers with Tunable Infrared Photoresponse

Alexander E. London,^a Lifeng Huang,^a Benjamin A. Zhang,^a M. Belen Oviedo,^b Joshua Tropp,^a Weichuan Yao,^c Zhenghui Wu,^c Bryan M. Wong,^b Tse Nga Ng,^c and Jason D. Azoulay^{a*}

^aSchool of Polymers and High Performance Materials, The University of Southern Mississippi, 118 College Drive #5050, Hattiesburg, Mississippi 39406, United States. ^bDepartment of Chemical & Environmental Engineering and Materials Science & Engineering, University of California Riverside, Riverside, California 92521, United States. ^cDepartment of Electrical and Computer Engineering, 9500 Gilman Drive, University of California San Diego, La Jolla, California 92093, United States.

*To whom correspondence should be addressed. e-mail: jason.azoulay@usm.edu

Computation. All DFT and TD-DFT calculations were carried out with the Gaussian 09 package (version C.01)¹ employing the B3LYP exchange-correlation functional² and a polarized 6-31G(d) basis set using default SCF convergence criteria (density matrix converged to at least 10^{-8}), DFT integration grid (75 radial and 302 angular quadrature points) and optimization convergence criteria (RMS force of at least 0.0003 Hartree/Bohr). The HOMO and LUMO figures for the **P2** and **P3** tetramers are shown in Figures S1-S4.

Table S1. Calculated data for (**P1–P5**) at the B3LYP/6-31G(d) level of theory.

| | HOMO ^a | LUMO ^a | E_g ^b | f ^c | E_g^{vert} ($n \rightarrow \infty$) ^d |
|------------------|-------------------|-------------------|--------------------|------------------|--|
| P1b ^e | -4.62 | -3.15 | 1.47 | 6.82 | 1.08 |
| P1 | -4.32 | -2.98 | 1.34 | 7.02 | 1.04 |
| P2 | -4.25 | -3.01 | 1.24 | 6.56 | 0.94 |
| P3 | -4.40 | -3.28 | 1.12 | 5.91 | 0.88 |
| P4 | -4.16 | -3.25 | 0.91 | 10.01 | 0.68 |
| P5 | -4.14 | -3.26 | 0.88 | 9.74 | 0.63 |

^aFrontier molecular orbital energies as determined at the at the B3LYP/6-31G(d) level of theory. ^bHOMO/LUMO orbital energy gap (E_g). ^cOscillator strength (f). ^d S_0 to S_1 vertical transition energy extrapolated to $n = \infty$ using the Kuhn equation ($E_g^{\text{vert}}(n \rightarrow \infty)$). All energies are in eV and oscillator strength is a unitless quantity. ^eData adopted from reference 3.

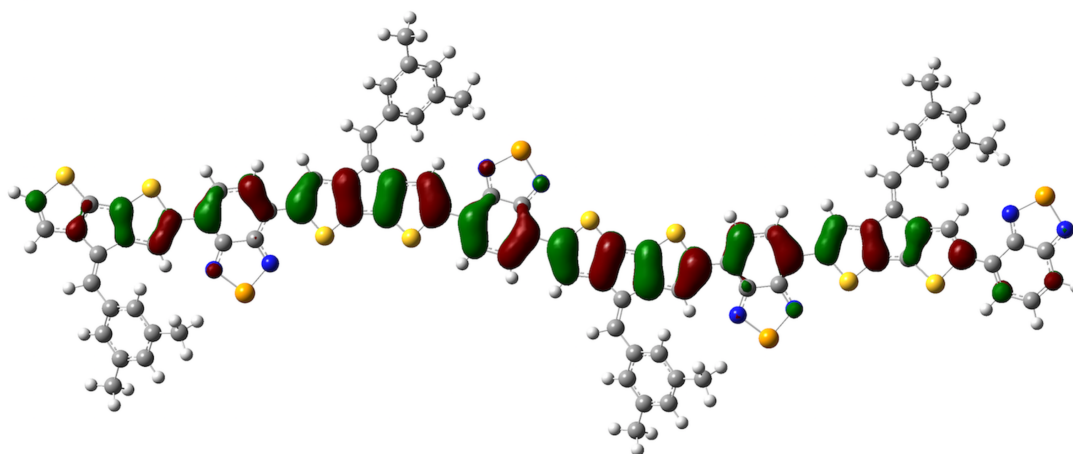


Figure S1. Optimized ground-state (S_0) geometric structures for the **P2** tetramer ($n = 4$) and pictorial representation of the HOMO wavefunction as determined at the B3LYP/6-31G(d) level of theory.

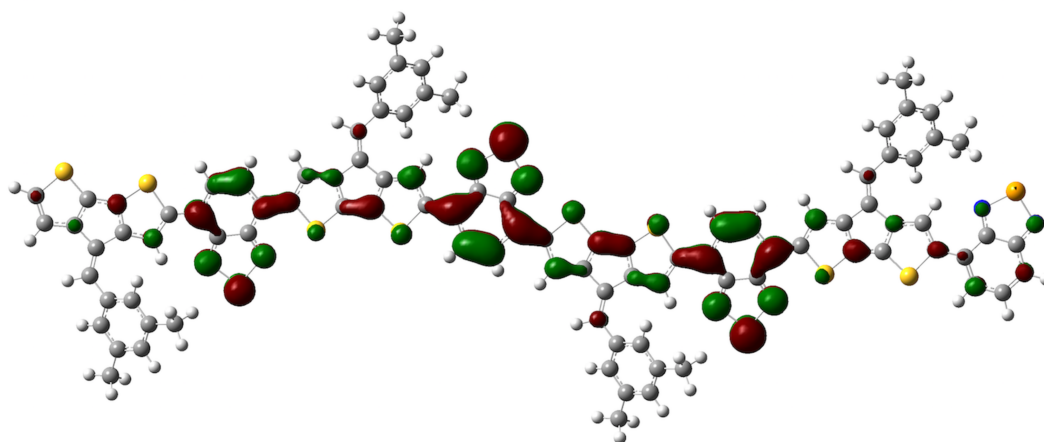


Figure S2. Pictorial representation of the LUMO wavefunction for the **P2** tetramer ($n = 4$) as determined at the B3LYP/6-31G(d) level of theory.

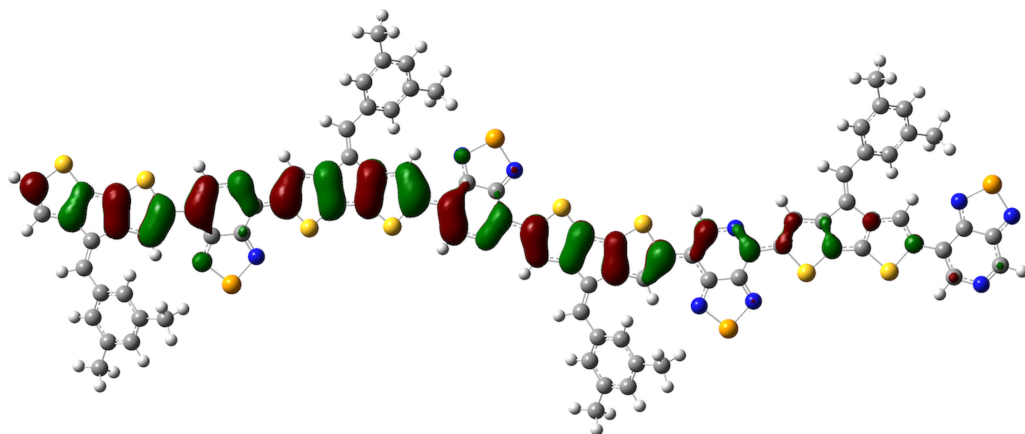


Figure S3. Optimized ground-state (S_0) geometric structures for the **P3** tetramer ($n = 4$) and pictorial representation of the HOMO wavefunction as determined at the B3LYP/6-31G(d) level of theory.

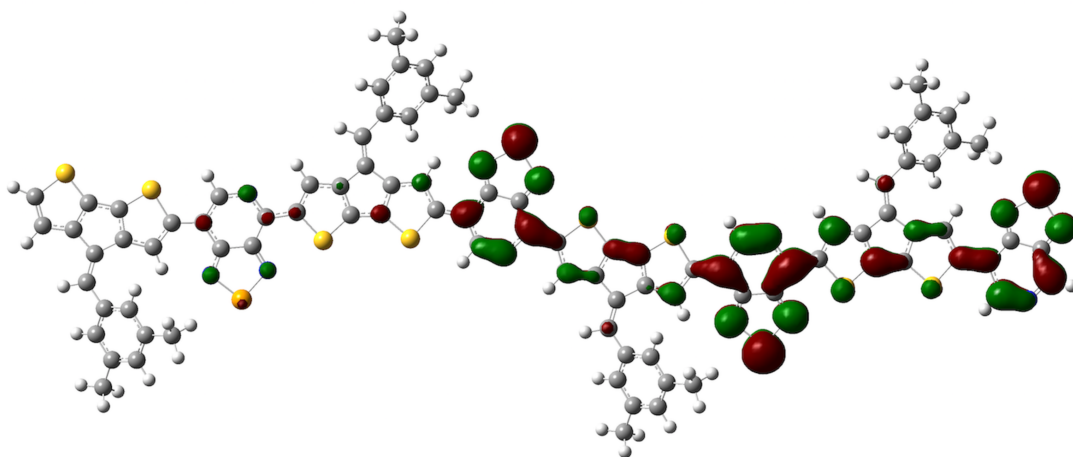


Figure S4. Pictorial representation of the LUMO wavefunction for the **P3** tetramer ($n = 4$) as determined at the B3LYP/6-31G(d) level of theory.

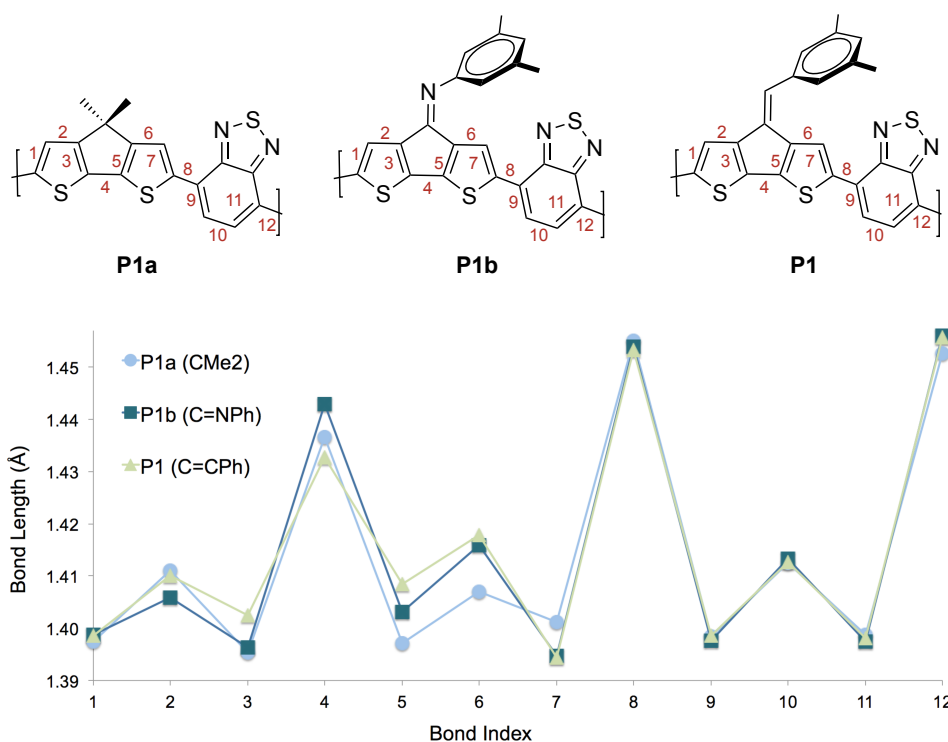


Figure S5. Repeat unit of **P1a**, **P1b**, and **P1** and bond length plots of the (central dimer) of the oligomers with $n = 6$ (C_1-C_{12} shown for clarity). Bond length values are in Å.

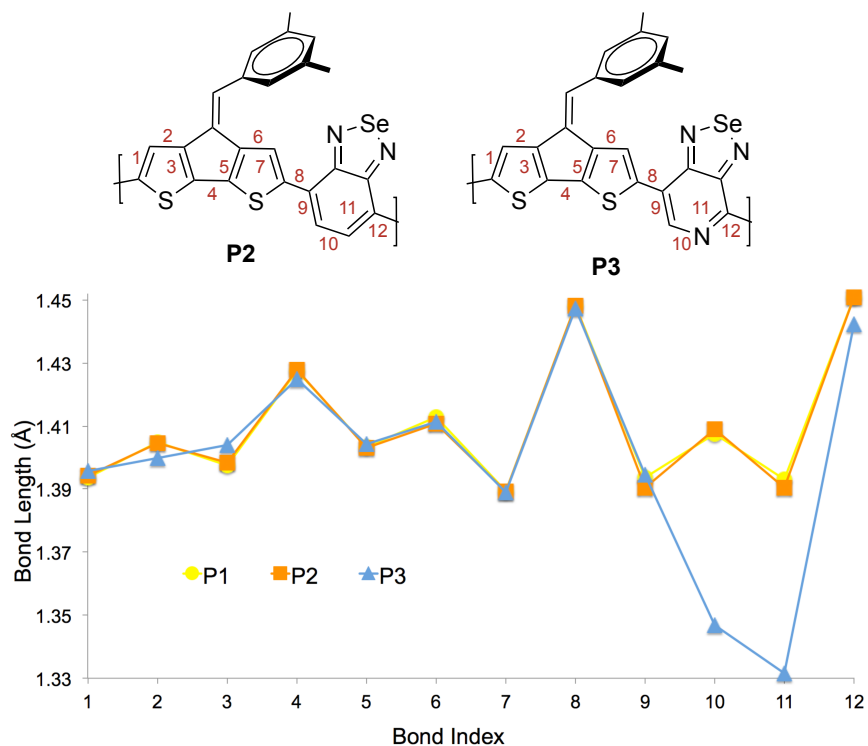


Figure S6. Repeat unit of **P1-P3** and bond length plots of the (central dimer) of the oligomers with $n = 6$ (C_1-C_{12} shown for clarity). Bond length values are in Å.

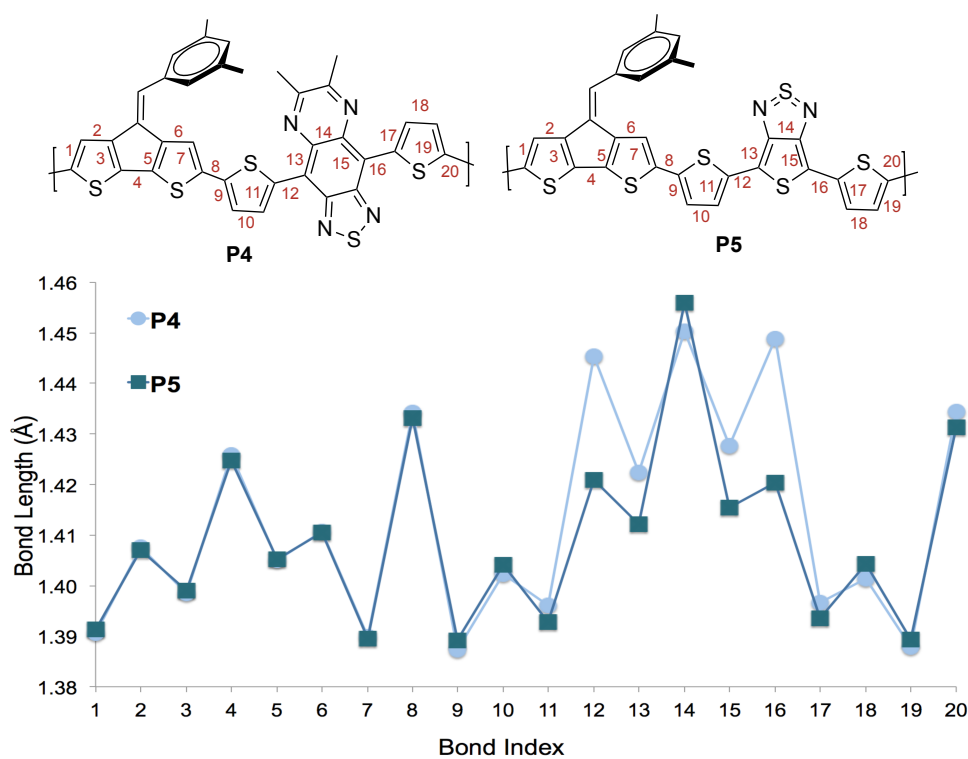


Figure S7. Repeat unit of **P4** and **P5** and bond length plots of the (central dimer) of the oligomers with $n = 6$ (C_1 - C_{20} shown for clarity). Bond length values are in Å.

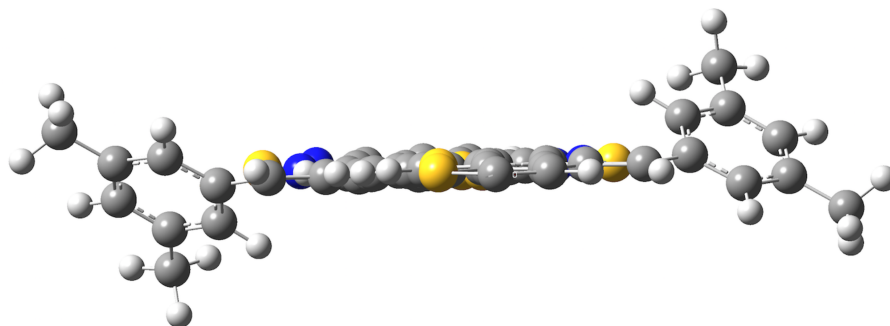


Figure S8. Side view of the optimized geometry of $(P1)_4$.

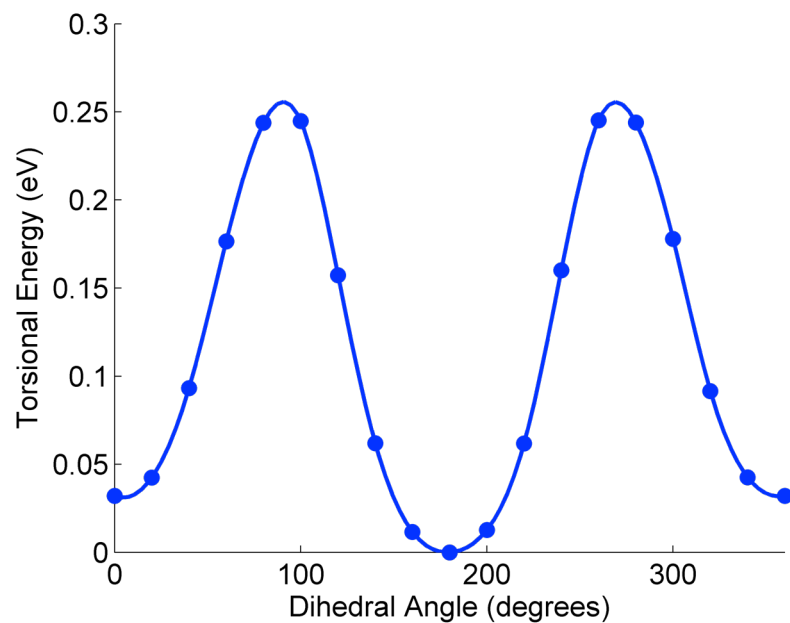


Figure S9. Torsional energy as a function of the dihedral angle for the **P1** dimer calculated at the B3LYP/6-31G(d) level of theory.

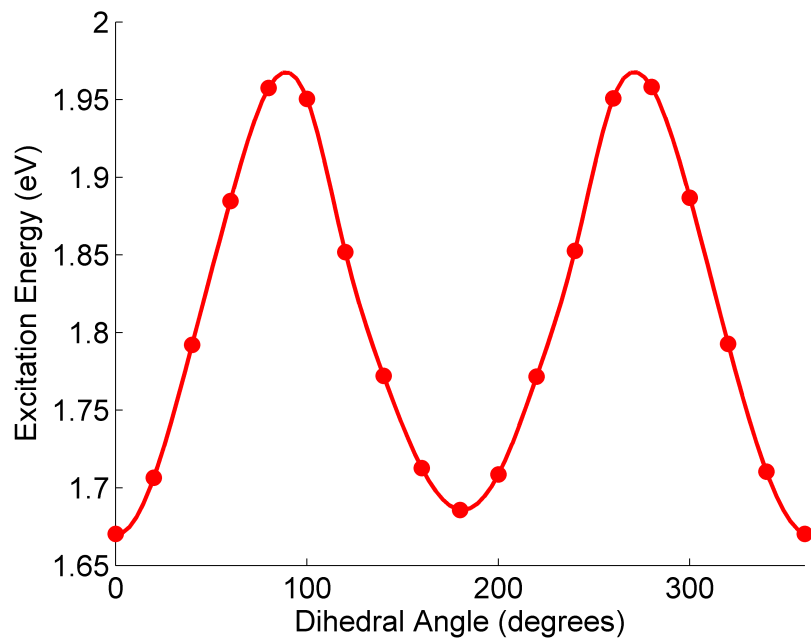


Figure S10. S₁ excitation energy as a function of the dihedral angle for the **P1** dimer calculated with time-dependent DFT at the B3LYP/6-31G(d) level of theory.

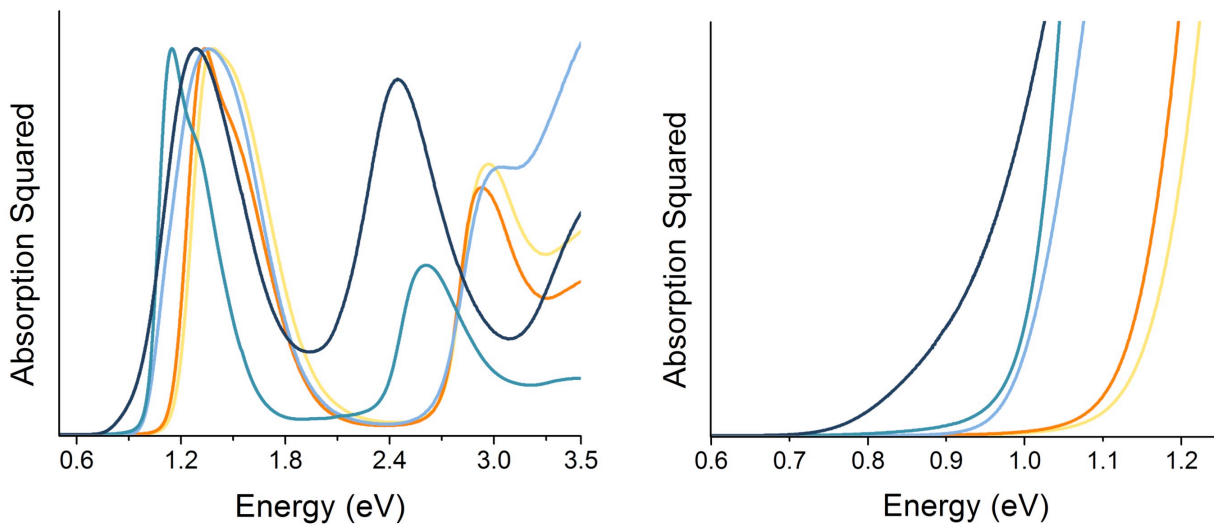


Figure S11. Absorption squared plots of **P1-P5** as thin films.

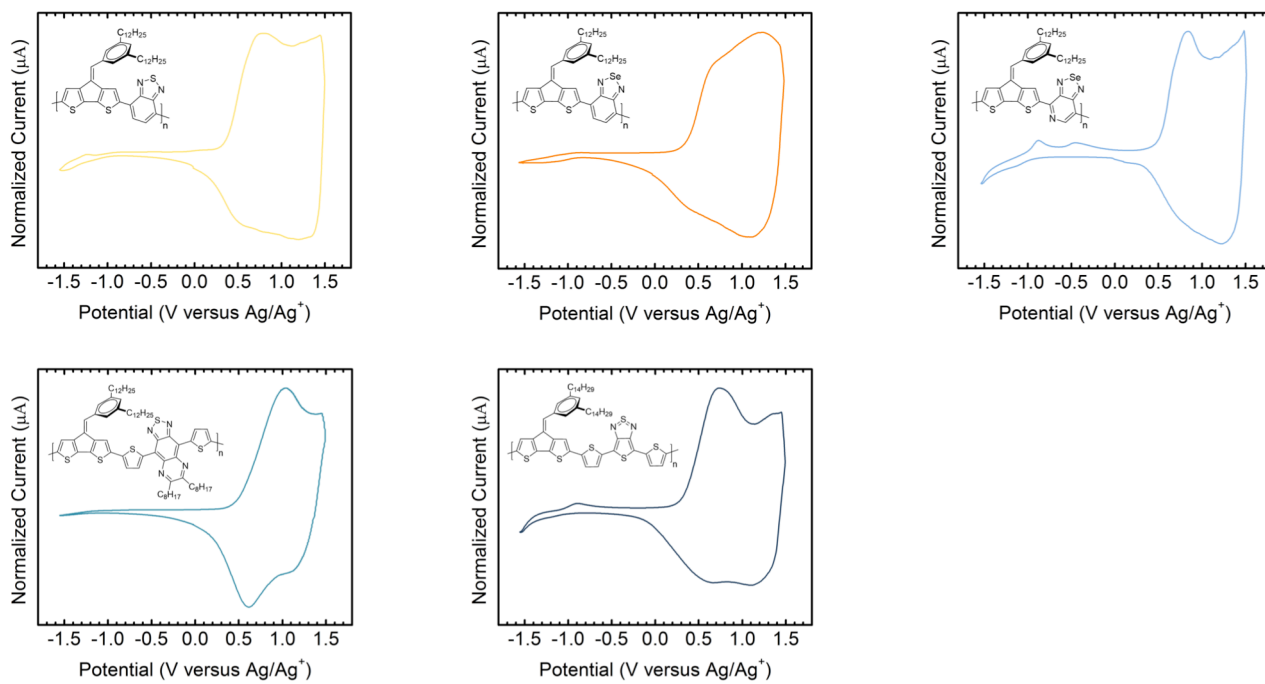


Figure S12. CV of **P1-P5** (third scan).

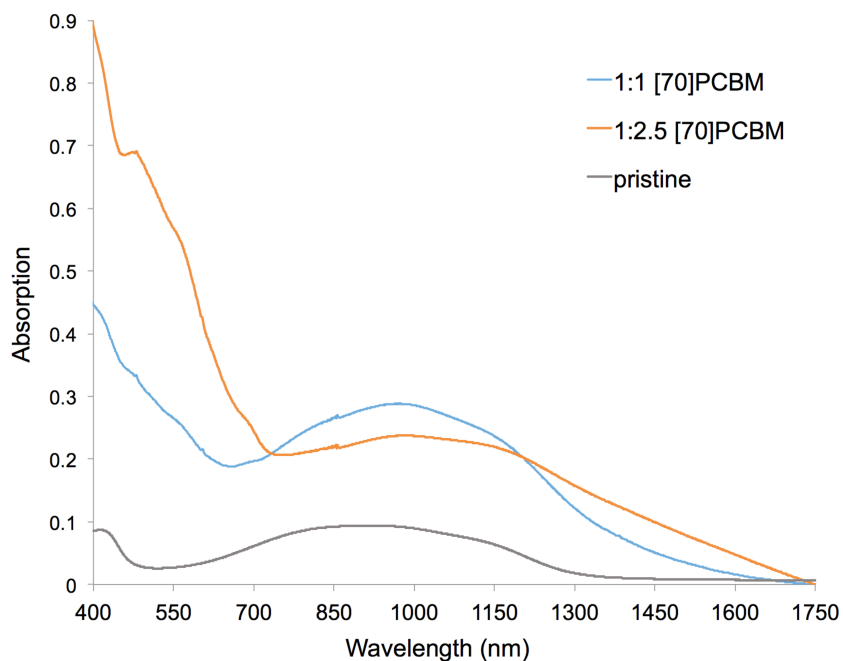


Figure S13. Absorption spectra of **P3** thin films with varying ratios of [70]PCBM.

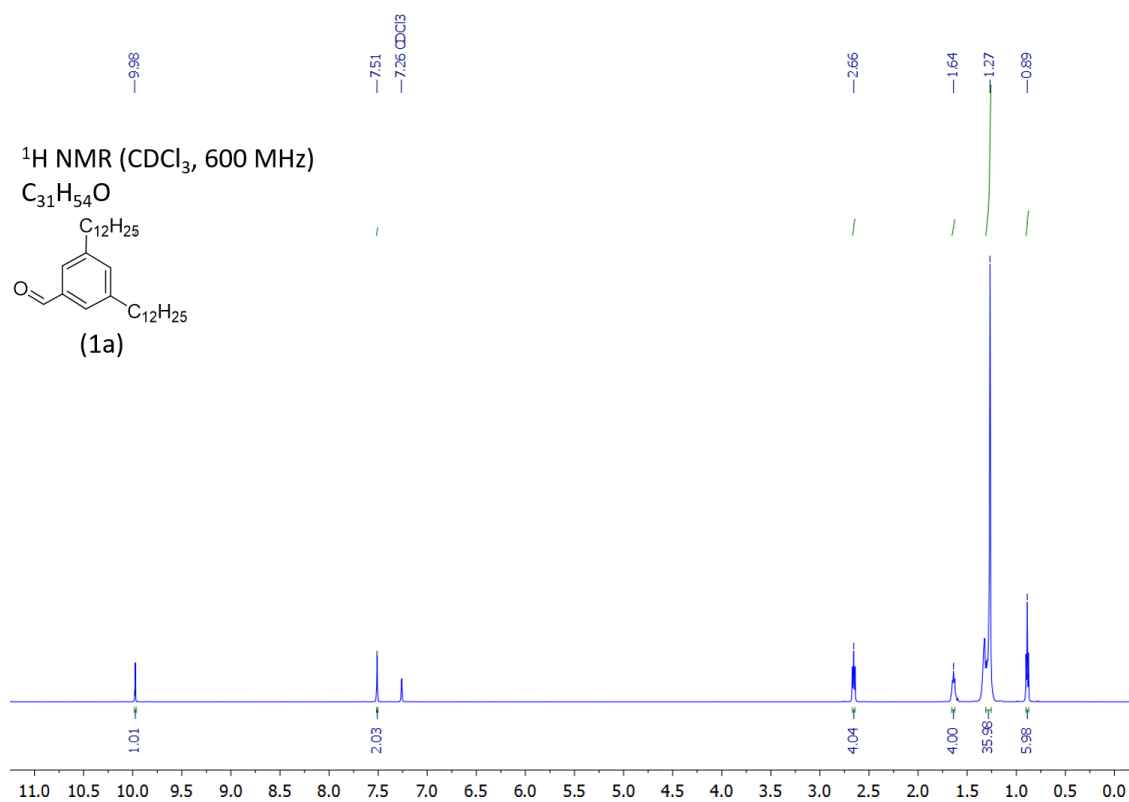


Figure S14. ¹H NMR spectra of **1a**.

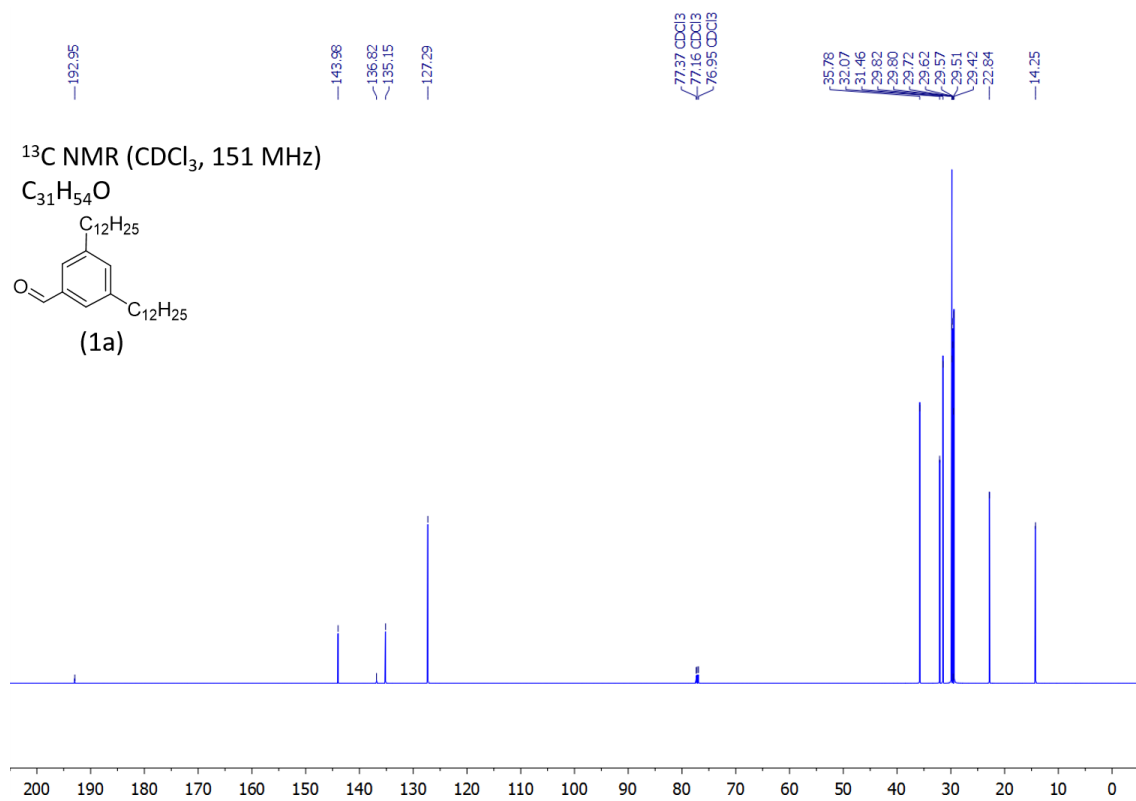


Figure S15. ^{13}C NMR spectra of **1a**.

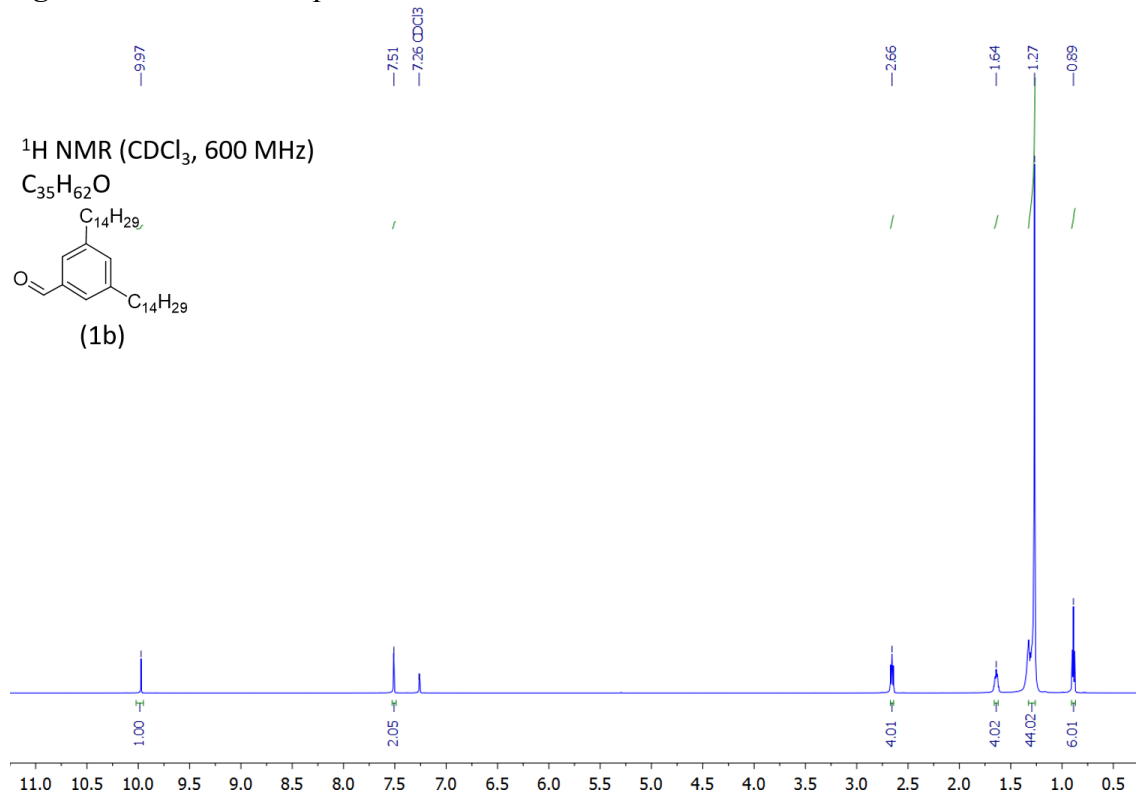


Figure S16. ^1H NMR spectra of **1b**.

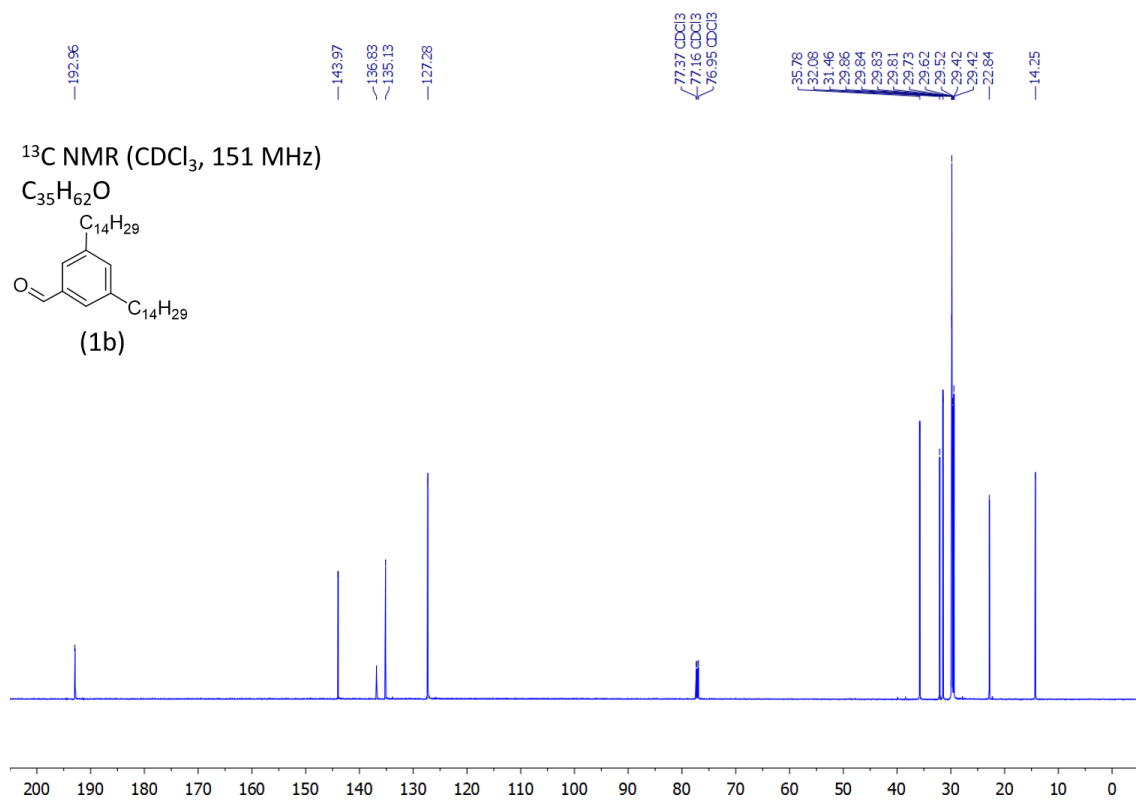


Figure S17. ^{13}C NMR spectra of 1b.

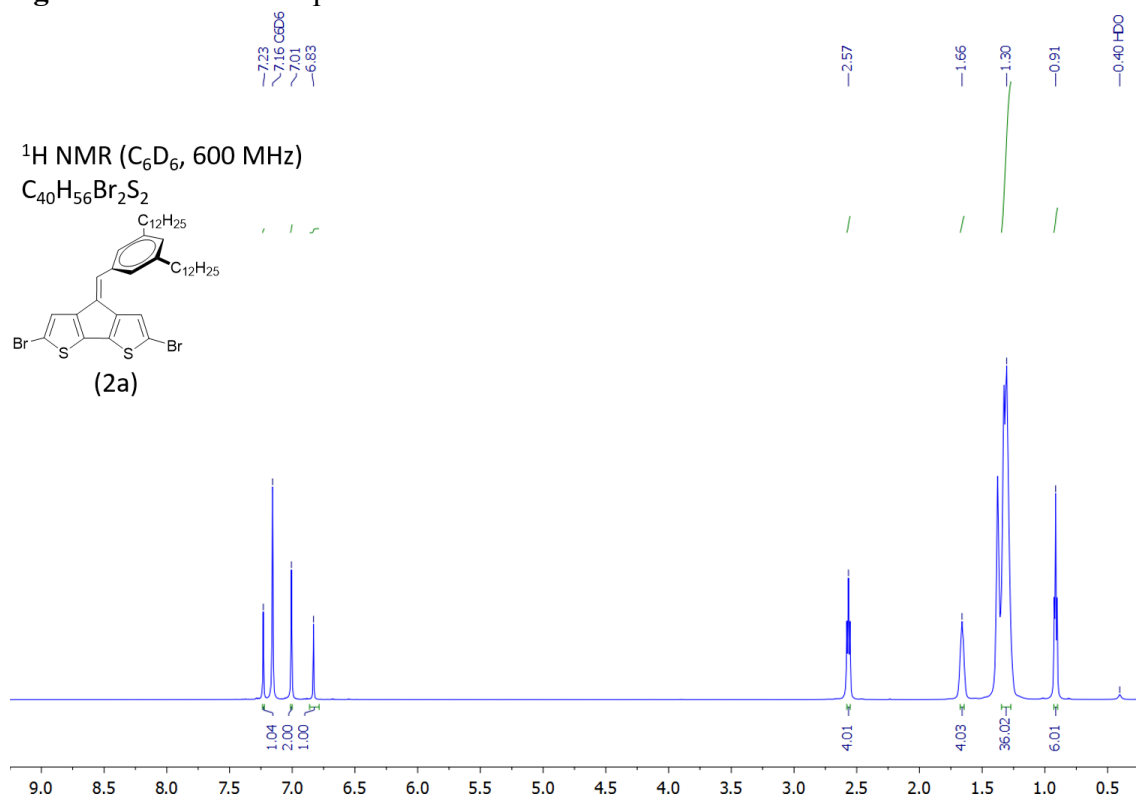


Figure S18. ^1H NMR spectra of 2a.

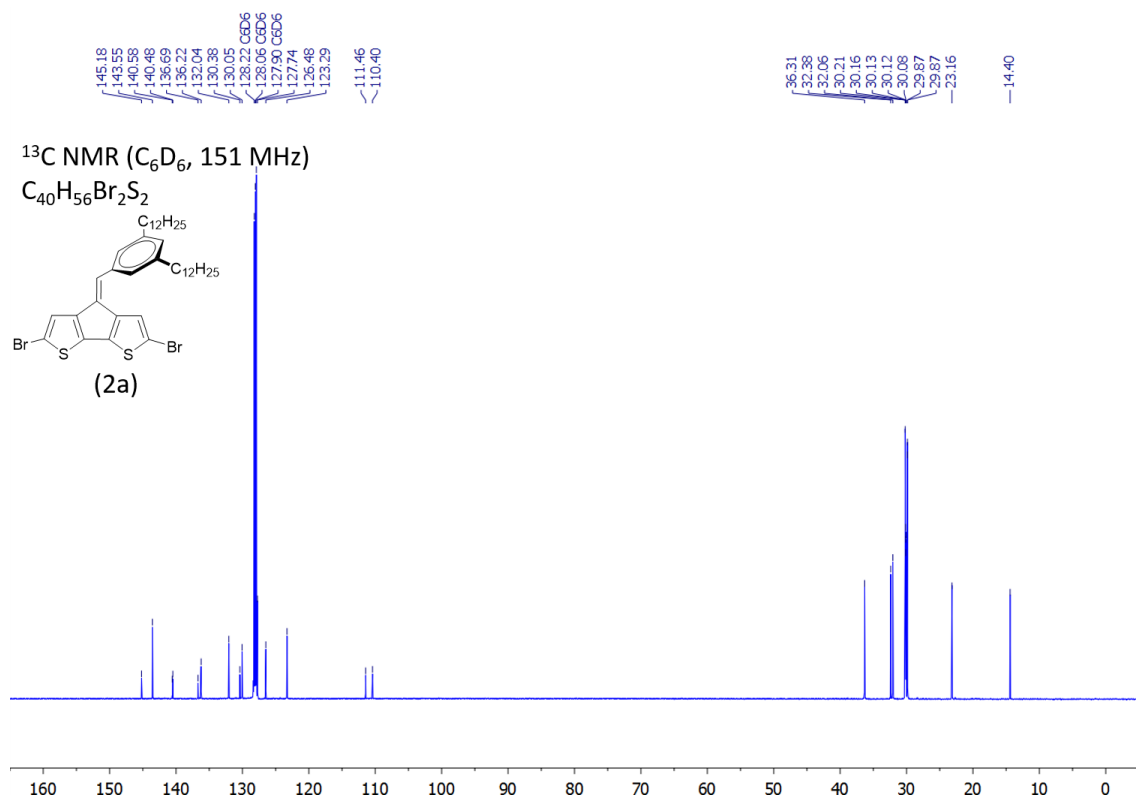


Figure S19. ¹³C NMR spectra of **2a**.

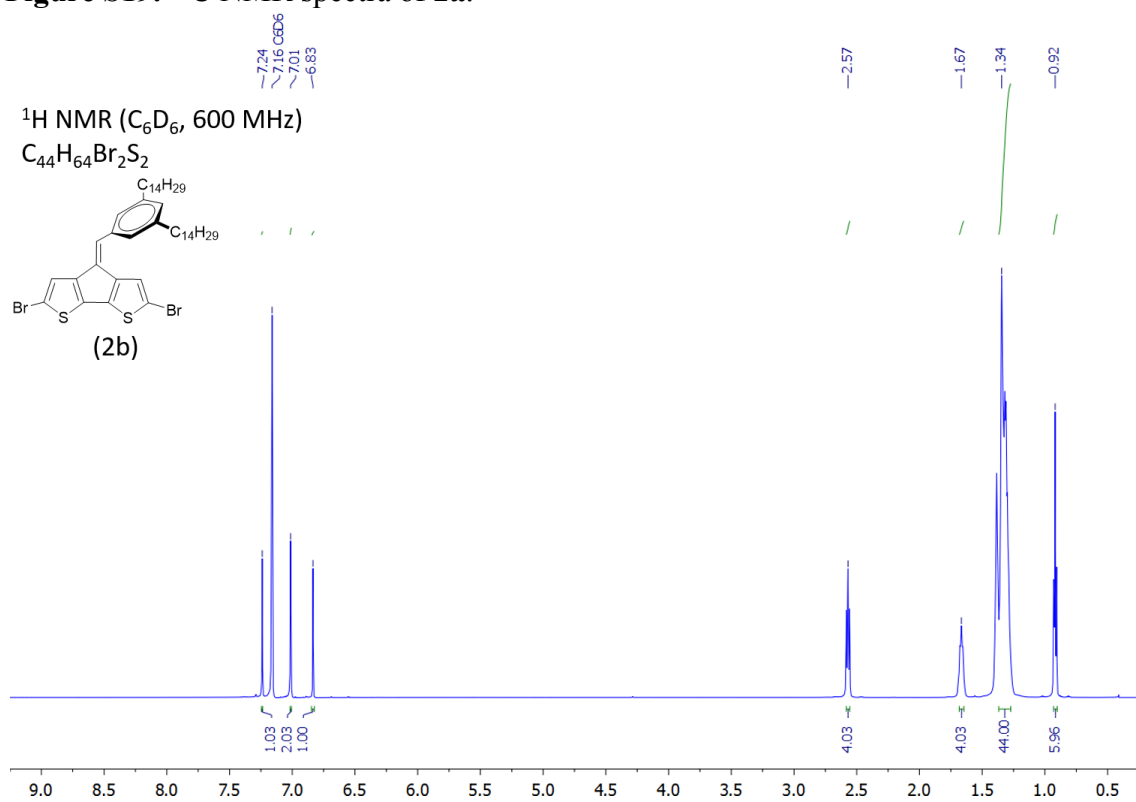


Figure S20. ¹H NMR spectra of **2b**.

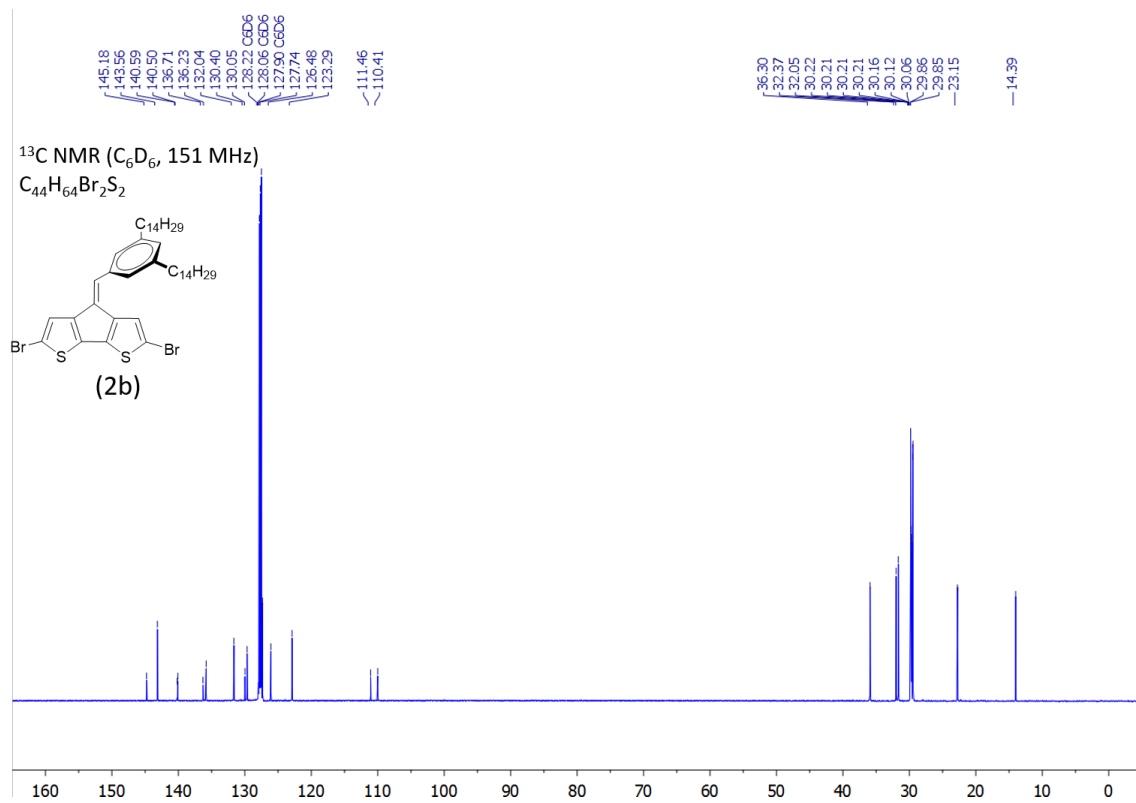


Figure S21. ¹³C NMR spectra of 2b.

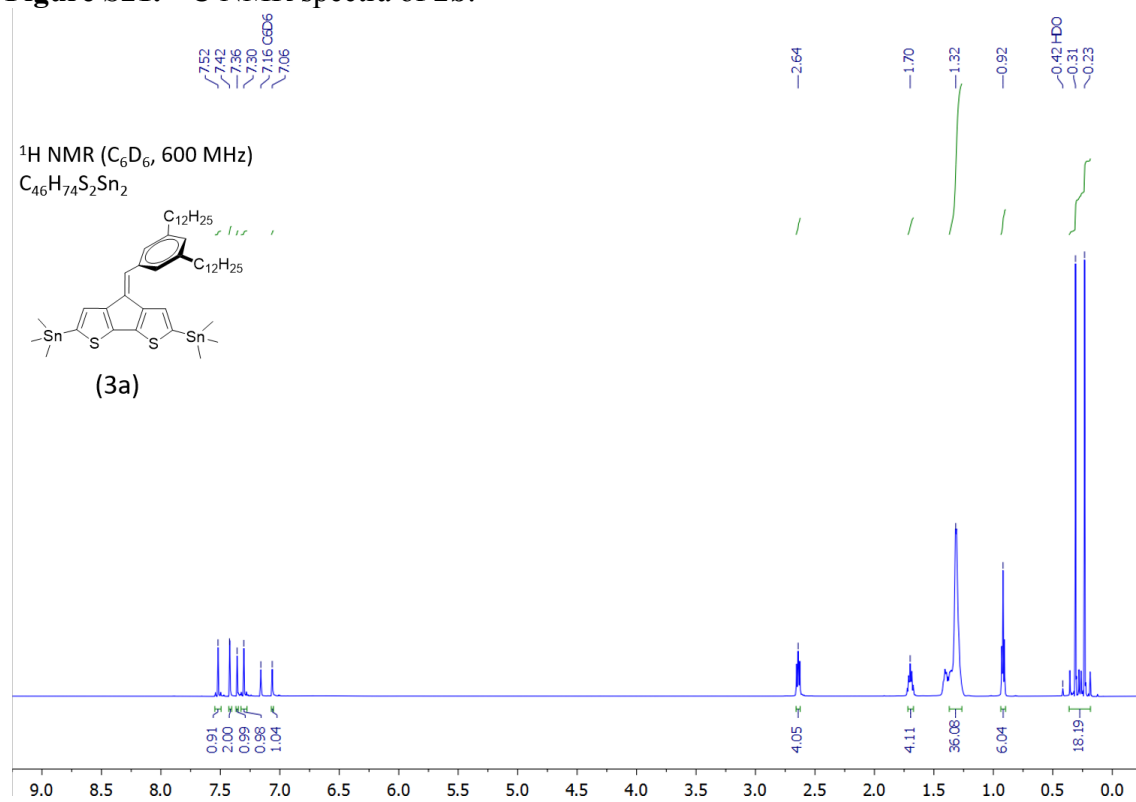


Figure S22. ¹H NMR spectra of 3a.

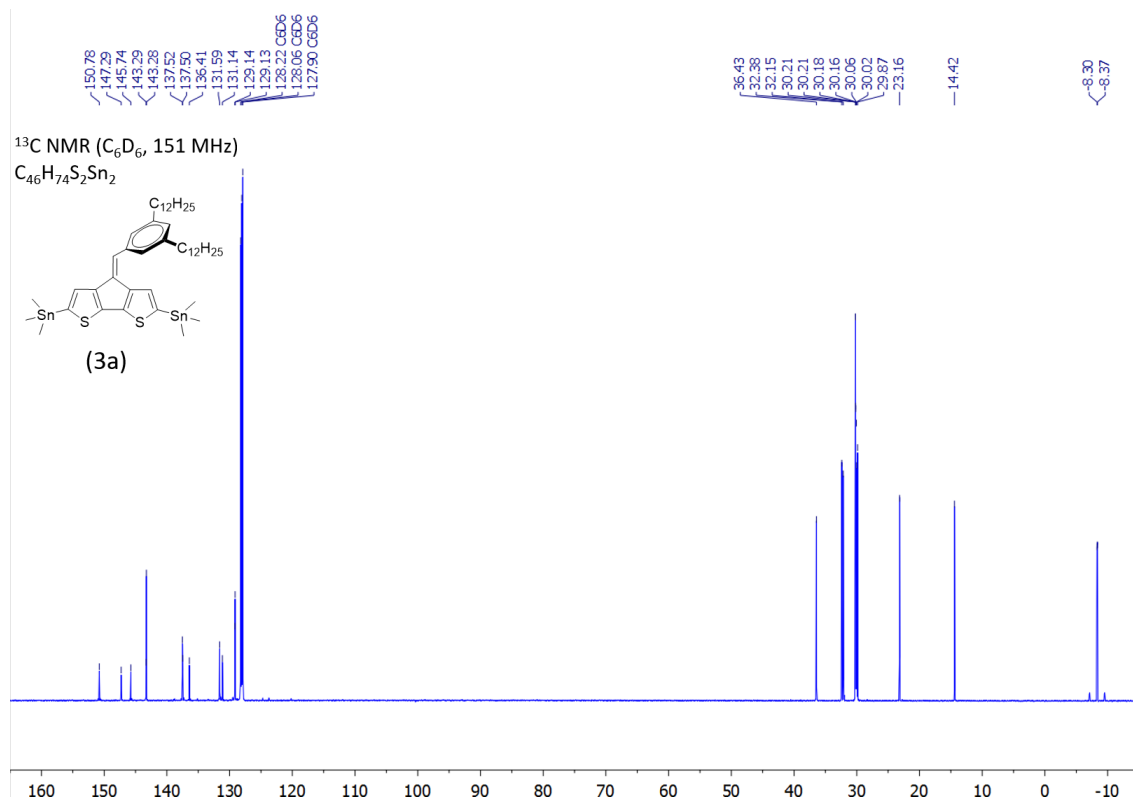


Figure S23. ^{13}C NMR spectra of **3a**.

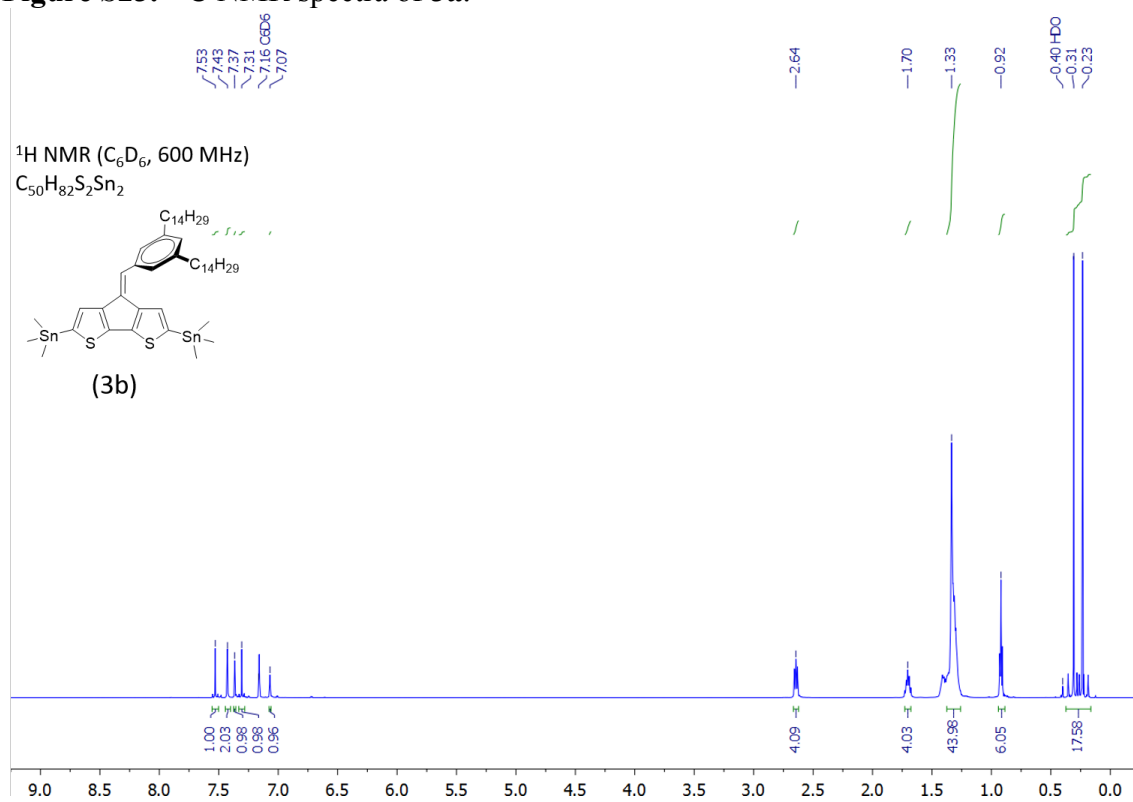


Figure S24. ^1H NMR spectra of **3b**.

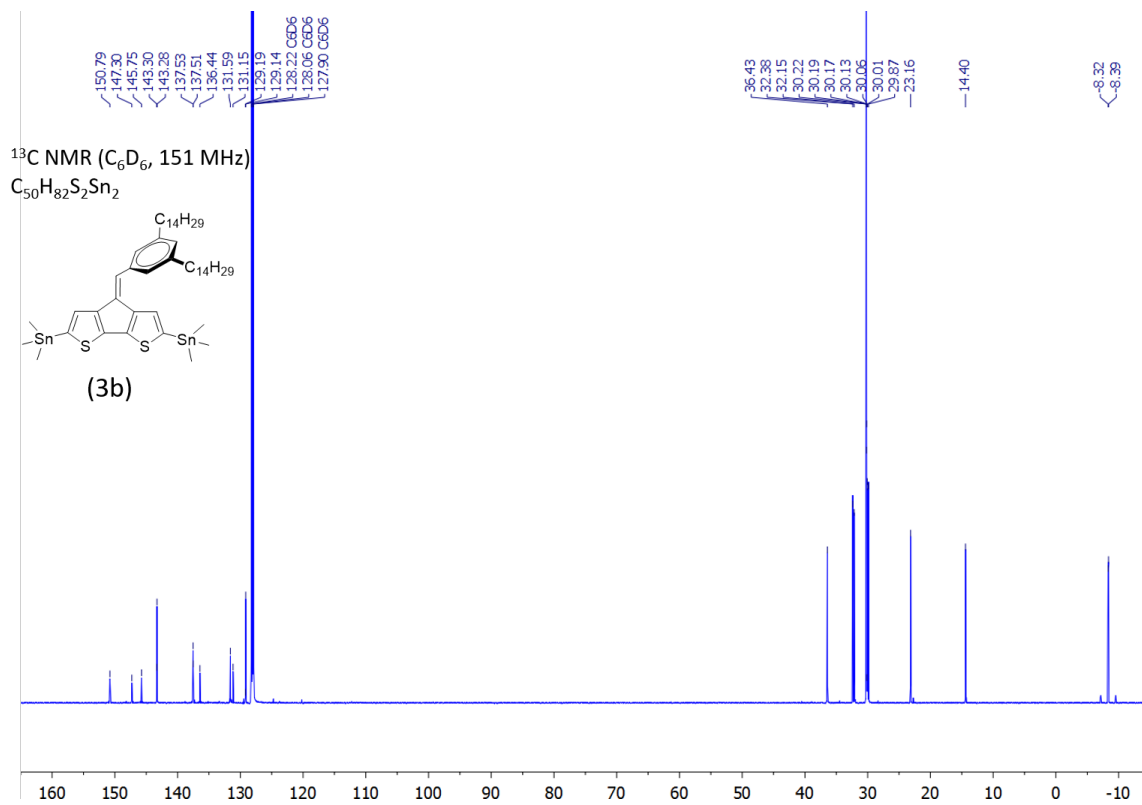


Figure S25. ^{13}C NMR spectra of **3b**.

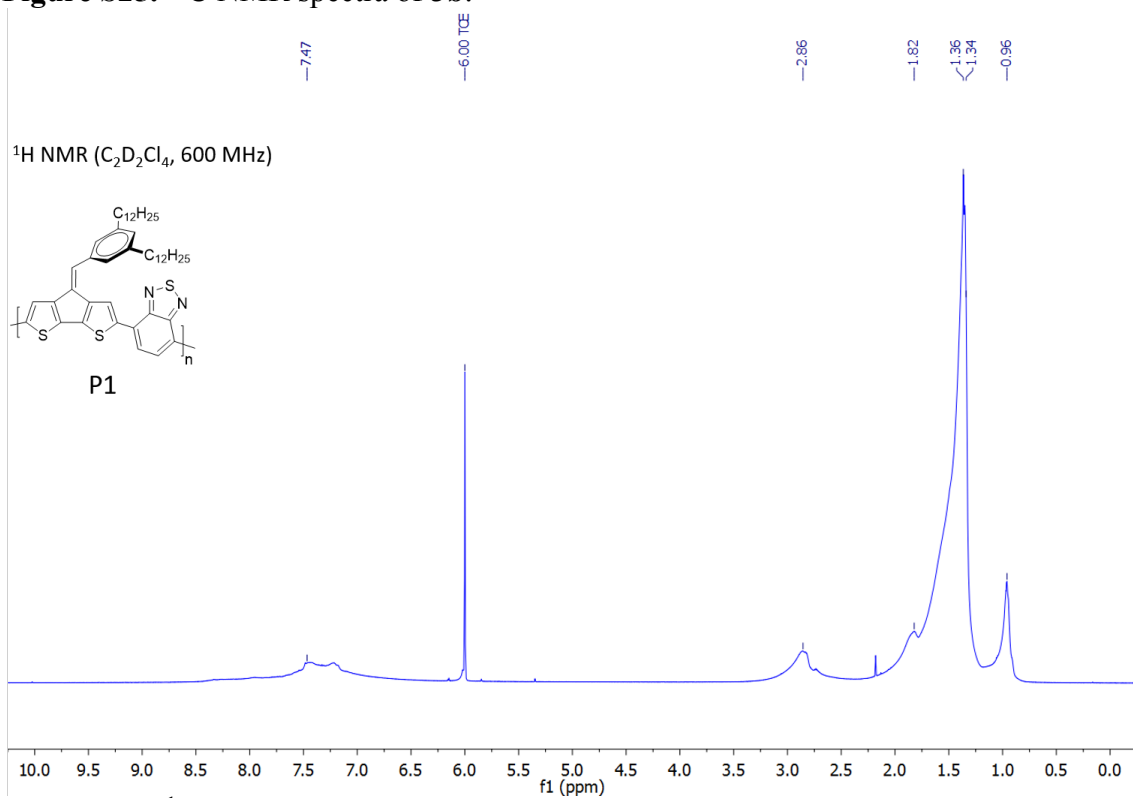


Figure S26. ^1H NMR spectra of **P1**.

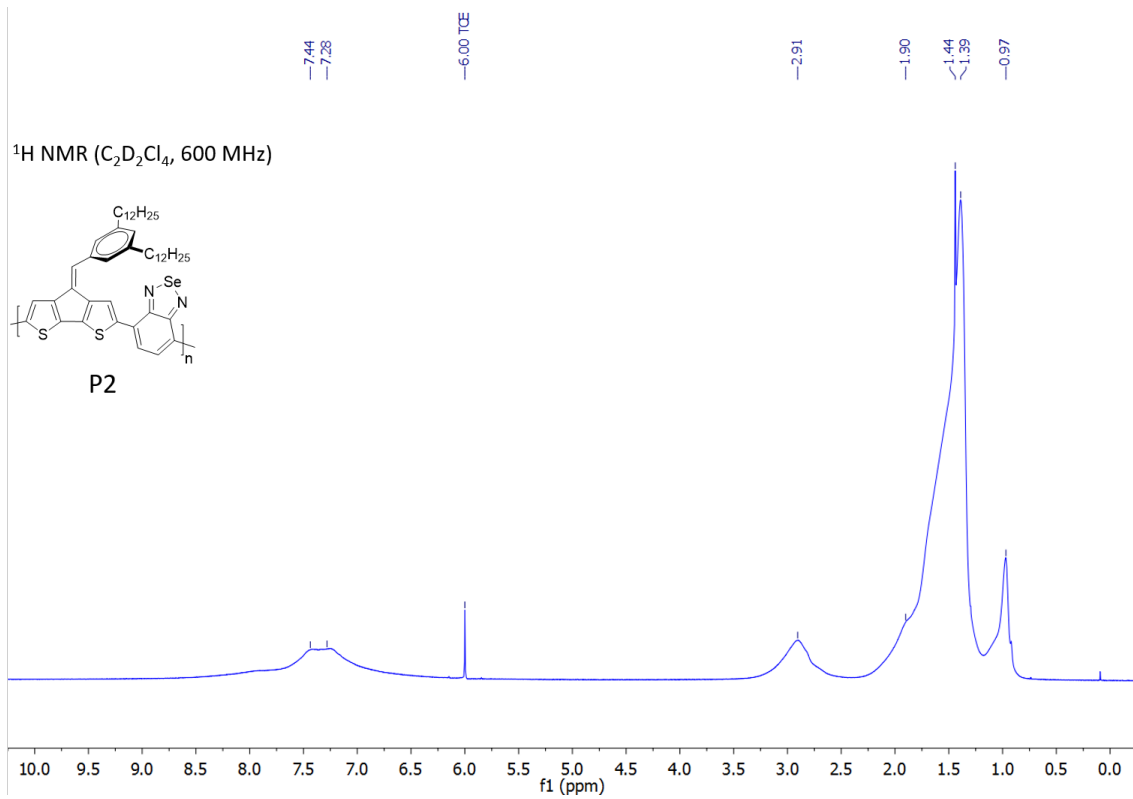


Figure S27. ^1H NMR spectra of P2.

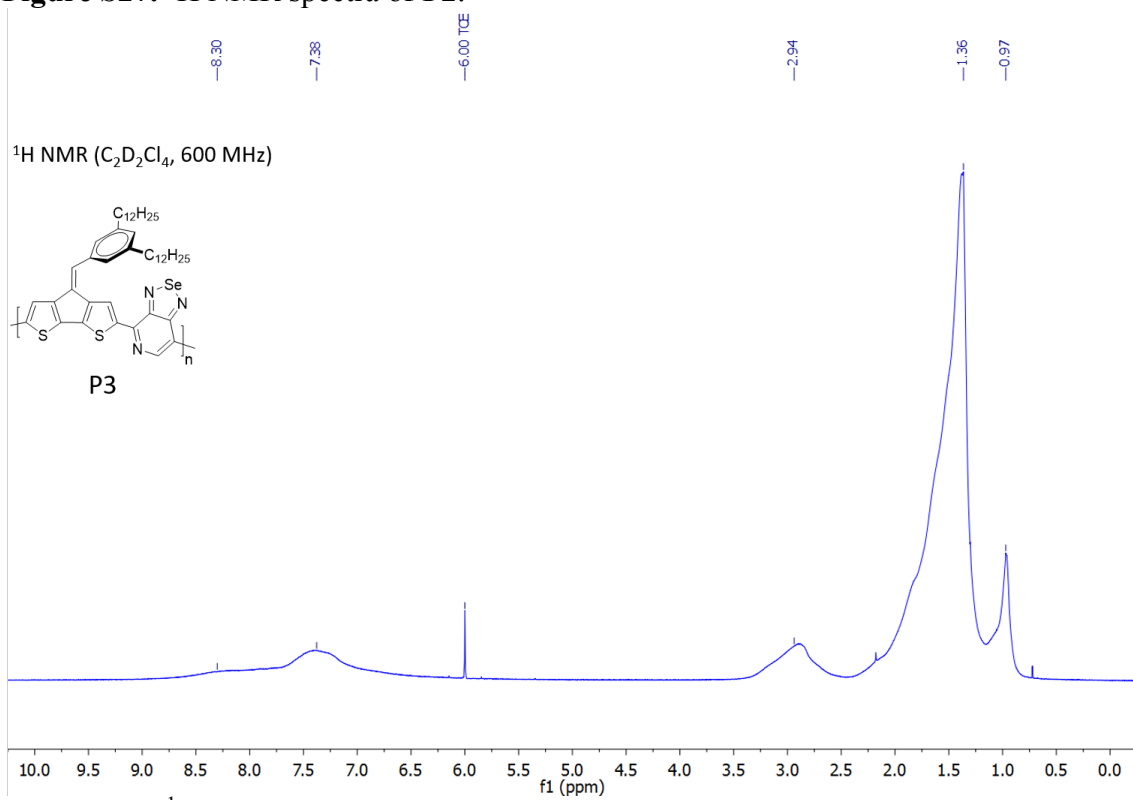


Figure S28. ^1H NMR spectra of P3.

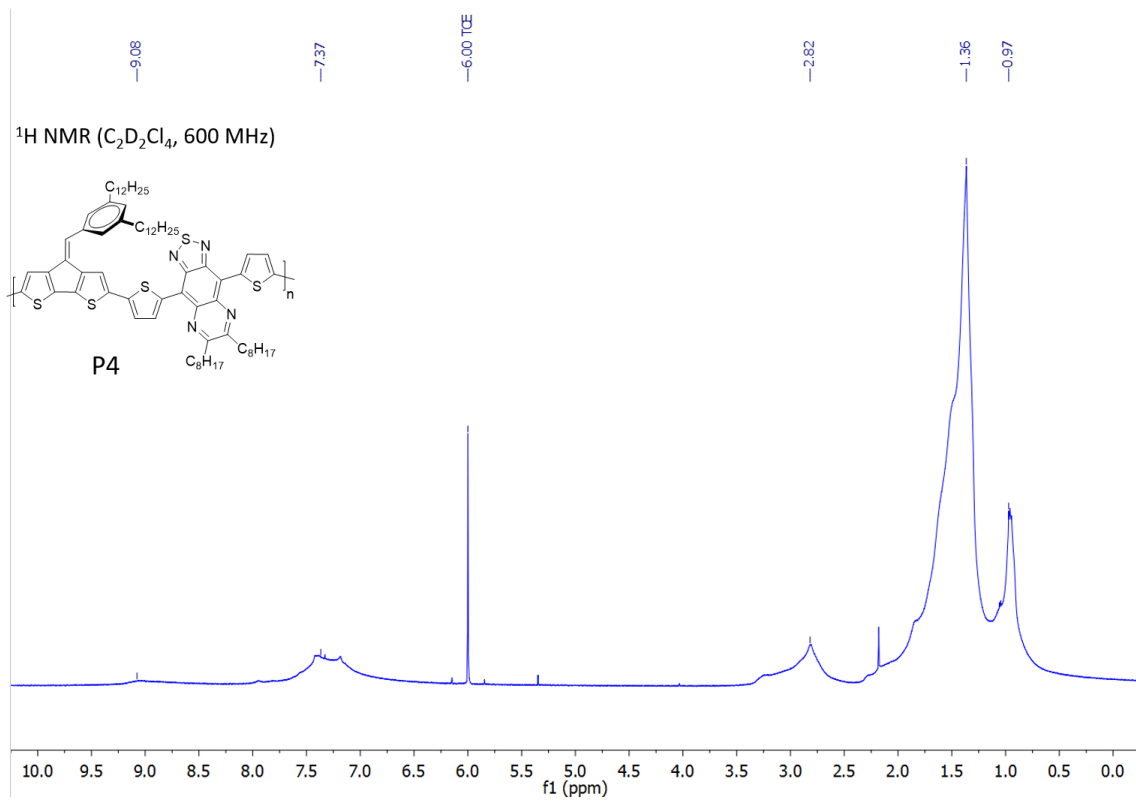


Figure S29. $^1\text{H NMR}$ spectra of **P4**.

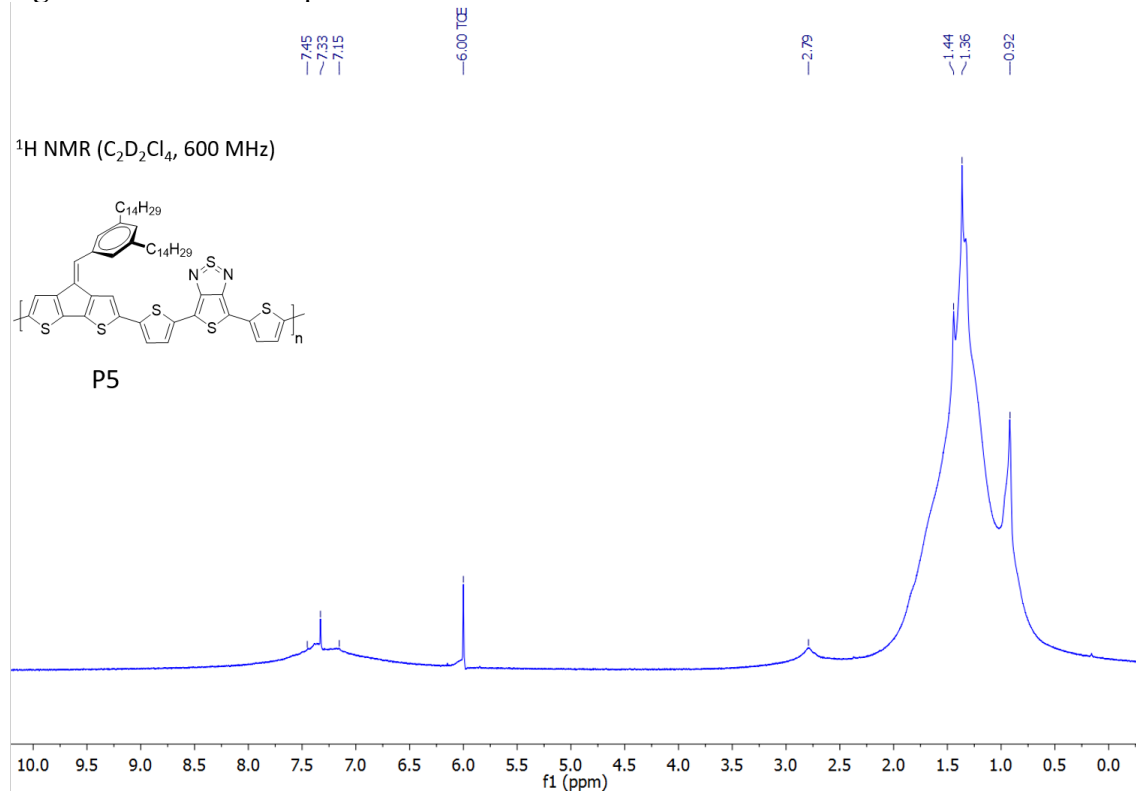


Figure S30. $^1\text{H NMR}$ spectra of **P5**.

References

1. Gaussian 09, Revision B.01, Frisch, M. J.; Trucks, G. W.; Schlegel, H. B.; Scuseria, G. E.; Robb, M. A.; Cheeseman, J. R.; Scalmani, G.; Barone, V.; Mennucci, B.; Petersson, G. A.; Nakatsuji, H.; Caricato, M.; Li, X.; Hratchian, H. P.; Izmaylov, A. F.; Bloino, J.; Zheng, G.; Sonnenberg, J. L.; Hada, M.; Ehara, M.; Toyota, K.; Fukuda, R.; Hasegawa, J.; Ishida, M.; Nakajima, T.; Honda, Y.; Kitao, O.; Nakai, H.; Vreven, T.; Montgomery, Jr., J. A.; Peralta, J. E.; Ogliaro, F.; Bearpark, M.; Heyd, J. J.; Brothers, E.; Kudin, K. N.; Staroverov, V. N.; Kobayashi, R.; Normand, J.; Raghavachari, K.; Rendell, A.; Burant, J. C.; Iyengar, S. S.; Tomasi, J.; Cossi, M.; Rega, N.; Millam, J. M.; Klene, M.; Knox, J. E.; Cross, J. B.; Bakken, V.; Adamo, C.; Jaramillo, J.; Gomperts, R.; Stratmann, R. E.; Yazyev, O.; Austin, A. J.; Cammi, R.; Pomelli, C.; Ochterski, J. W.; Martin, R. L.; Morokuma, K.; Zakrzewski, V. G.; Voth, G. A.; Salvador, P.; Dannenberg, J. J.; Dapprich, S.; Daniels, A. D.; Farkas, Ö.; Foresman, J. B.; Ortiz, J. V.; Cioslowski, J.; Fox, D. J. Gaussian, Inc., Wallingford CT, 2009.
2. A.D. Becke, *J. Chem. Phys.*, **1993**, *98*, 5648-5652.
3. M. E. Foster, B. A. Zhang, D. Murtagh, Y. Liu, M. Y. Sfeir, B. M. Wong and J. D. Azoulay, *Macromol. Rapid Commun.*, **2014**, *35*, 1516-1521.